UC San Diego

UC San Diego Previously Published Works

Title

Pushing the limits of ultrafast diffraction: Imaging quantum coherences in isolated molecules.

Permalink

https://escholarship.org/uc/item/82k4b37n

Journal

iScience, 27(9)

Authors

Tang, Zilong

Jarupula, Ramesh

Yong, Haiwang

Publication Date

2024-09-20

DOI

10.1016/j.isci.2024.110705

Peer reviewed

eScholarship.org Powered by the California Digital Library
University of California

iScience

CellPress
OPEN ACCESS

Perspective

Pushing the limits of ultrafast diffraction: Imaging quantum coherences in isolated molecules

Zilong Tang,[1] Ramesh Jarupula,[1] and Haiwang Yong[1,2,*]

SUMMARY

Quantum coherence governs the outcome and efficiency of photochemical reactions and ultrafast molecular dynamics. Recent ultrafast gas-phase X-ray scattering and electron diffraction have enabled the observation of femtosecond nuclear dynamics driven by vibrational coherence. However, probing attosecond electron dynamics and coupled electron-nuclear dynamics remains challenging. This article discusses advances in ultrafast X-ray scattering and electron diffraction, highlighting their potential to resolve attosecond charge migration and vibronic coupling at conical intersections. Novel techniques, such as X-ray scattering with orbital angular momentum beams and combined X-ray and electron diffraction, promise to selectively probe coherence contributions and visualize charge migration in real-space. These emerging methods could further our understanding of coherence effects in chemical reactions.

INTRODUCTION

Quantum coherence plays a crucial role in determining the outcome and efficiency of photochemical reactions and ultrafast dynamics.[1,2] This quantum phenomenon manifests in molecules in three distinct yet interconnected forms.

Vibrational coherences

Arising from superpositions of vibrational states, these coherences involve energy gaps typically ranging from ten to a few hundred millielectronvolt (meV). This corresponds to nuclear motions on the femtosecond timescale.

Electronic coherences

Generated by superpositions of multiple electronic states with larger energy gaps compared to vibrational states, typically on the order of 1–10 eV. These result in rapid electron dynamics in molecules with coherence periods ranging from sub-femtoseconds to attoseconds.

Vibronic coherences

Resulting from the coupling of both electronic and vibrational degrees of freedom, involving energy gaps that span a wide range. One important example in molecular systems is conical intersections (CIs), where two or more adiabatic potential energy surfaces become degenerate, resulting in strong non-adiabatic couplings. These couplings play critical roles in virtually all reaction dynamics, such as light-induced isomerization, charge transfer, and energy transfer.

To fully understand the role of quantum coherence in chemical reactions, it is essential to resolve all these forms in real space and time as the reaction occurs. This requires a comprehensive understanding of both nuclear and electronic dynamics, particularly the coupled electronic and nuclear motions. Unraveling the interplay between these different manifestations of quantum coherence and their impact on chemical reactions has the potential to revolutionize our understanding of chemical processes and advance quantum computing technologies.[3–5]

The nuclear motion of molecules, specifically the role of vibrational coherences in chemical reactions, has been extensively investigated in recent years. Traditionally, molecular structures have been determined using X-ray crystallography and electron diffraction on crystalline samples. The development of time-resolved gas-phase X-ray and electron diffraction techniques has opened new avenues for investigating the structural dynamics of isolated molecules on picosecond timescales.[6–10] By employing pump-probe schemes with ultrafast laser pulses, the real-time dynamics of chemical reactions, including transition states,[11–13] can be captured with atomic spatial resolution. Recent advancements in ultrafast gas-phase X-ray scattering and mega-electron-volt ultrafast electron diffraction (MeV-UED) have further pushed the boundaries of temporal and spatial resolution,[14–18] enabling the tracking of femtosecond atomic nuclear motion in molecules governed by vibrational coherence.

[1]Department of Chemistry and Biochemistry, University of California, San Diego, La Jolla, CA 92093, USA
[2]Program in Materials Science and Engineering, University of California, San Diego, La Jolla, CA 92093, USA
*Correspondence: hyong@ucsd.edu
https://doi.org/10.1016/j.isci.2024.110705

This is an open access article under the CC BY-NC-ND license (http://creativecommons.org/licenses/by-nc-nd/4.0/).

Despite recent progress in studying vibrational coherences in molecules, the direct observation of attosecond electron dynamics originating from purely electronic coherences and coupled electron-nuclear dynamics arising from vibronic coherences remains a challenge. Purely electronic coherences can lead to attosecond charge migration and energy transfer processes within the molecule, which play essential roles in photochemical reactions and light-harvesting systems. While recent ultrafast spectroscopic studies have begun to shed light on these attosecond electron dynamics,[19–24] capturing these phenomena with diffraction methods has not been achieved, mainly due to the lack of required attosecond temporal resolutions. This is expected to become possible in the near future with ongoing efforts to develop attosecond X-ray free-electron lasers (XFELs) and attosecond electron pulses.[25–29] Furthermore, experimental signatures of vibronic coherences are often overshadowed by stronger signals originating from electronic populations or vibrational excitations, necessitating novel experimental concepts and theoretical methods to distinguish these subtle coherent phenomena amidst complex molecular dynamics.

This perspective aims to provide a brief overview of the current state-of-the-art ultrafast gas-phase X-ray scattering and electron diffraction techniques, particularly their experimental advances in studying nuclear dynamics driven by vibrational coherence. By discussing recent advances and future opportunities in extending these techniques to investigate the other two forms of quantum coherences (i.e., electronic and vibronic coherences), we hope to inspire the development of new experimental and theoretical approaches that can provide a comprehensive understanding of all three forms of quantum coherences in photoinduced processes. Such advancements could lead to the ability to directly observe and control attosecond electron dynamics as well as coupled electron-nuclear dynamics at conical intersections. The question of how to control quantum coherences in molecules to influence reaction outcomes has led to the emergence of a new field called "attochemistry."[30,31] This emerging field has potential far-reaching applications in areas such as photocatalysis, light-harvesting, and quantum sensing.[32–34]

THEORY OF COHERENCE SIGNALS IN TIME-RESOLVED MOLECULAR DIFFRACTION

Time-resolved diffraction techniques have emerged as powerful tools for probing the quantum dynamics of molecules with unprecedented spatial and temporal resolution. The theoretical description of time-resolved molecular diffraction has been extensively studied in the 1990s by Wilson, Cao, and co-workers.[35–37] It has been revealed lately that in addition to the well-known elastic and inelastic scattering components, time-resolved diffraction signals contain distinct contributions related to electronic coherence.[38–42] Such coherence signal, arising from the superposition of electronic (or vibronic) states, plays a crucial role in the ultrafast dynamics of molecules, such as charge migration and conical intersection passage. By probing the time evolution of the coherence signal, time-resolved diffraction techniques can provide new insights into the fundamental quantum processes that govern chemical reactivity. In this section, we present a brief overview of the time-resolved diffraction theory, with an emphasis on its connection to the quantum coherences in molecules.

The time-dependent molecular many-electron wavefunction prepared by a pump pulse may be expanded as

$$\Psi(\mathbf{r},\mathbf{R},t) = \sum_i c_i(t)\chi_i(\mathbf{R},t)\varphi_i(\mathbf{r},\mathbf{R}) \qquad \text{(Equation 1)}$$

where i labels the adiabatic electronic states, $\chi_i(\mathbf{R},t)$ is the normalized nuclear wavepacket in the adiabatic electronic state $\phi_i(\mathbf{r},\mathbf{R})$, r and R are the electronic and nuclear coordinates, t is time and c_i is the electronic state amplitude.

Using Equation 1, the time-evolving electronic charge density in real space is given by

$$\sigma^{\mathrm{E}}_{\mathrm{tot}}(\mathbf{r},t) = \sum_{ij}\rho_{ji}(t)\left\langle\chi_i(t)\middle|\hat{\sigma}^{\mathrm{E}}_{ij}(\mathbf{r})\middle|\chi_j(t)\right\rangle$$

$$= \sum_i \rho_{ii}(t)\left\langle\chi_i(t)\middle|\hat{\sigma}^{\mathrm{E}}_{ii}(\mathbf{r})\middle|\chi_i(t)\right\rangle + 2\Re\left[\sum_{j>i}\rho_{ji}(t)\left\langle\chi_i(t)\middle|\hat{\sigma}^{\mathrm{E}}_{ij}(\mathbf{r})\middle|\chi_j(t)\right\rangle\right]$$

$$= \sigma^{\mathrm{E}}_{\mathrm{pop}}(\mathbf{r},t) + \sigma^{\mathrm{E}}_{\mathrm{coh}}(\mathbf{r},t) \qquad \text{(Equation 2)}$$

Here $\hat{\sigma}^{\mathrm{E}}(\mathbf{r})$ is the electronic charge-density operator, ρ is the density matrix operator, $\rho_{ii}(t) = c_i^*(t)c_i(t)$ are real numbers representing the electronic populations at time t while the coherence terms, $\rho_{ji}(t) = c_i^*(t)c_j(t)$ with $j \neq i$, consists of complex numbers. The vibronic coherence is obtained from the combined electronic-nuclear wavefunction as the overlap of the nuclear wave packets. The total electronic charge density contains contributions from both time-evolving electronic population density $\sigma^{\mathrm{E}}_{\mathrm{pop}}(\mathbf{r},t)$ and coherent density $\sigma^{\mathrm{E}}_{\mathrm{coh}}(\mathbf{r},t)$.

For the case of attosecond electron dynamics in molecules where the nuclei are static, the $\sigma^{\mathrm{E}}_{\mathrm{tot}}(\mathbf{r},t)$ in Equation 2 can be simplified as

$$\sigma^{\mathrm{E}}_{\mathrm{tot}}(\mathbf{r},t) = \sigma^{\mathrm{E}}_{\mathrm{pop}}(\mathbf{r}) + \sigma^{\mathrm{E}}_{\mathrm{coh}}(\mathbf{r},t) = \sum_i \rho_{ii}\sigma^{\mathrm{E}}_{ii}(\mathbf{r}) + \sum_{i\neq j}\rho_{ji}(t)\sigma^{\mathrm{E}}_{ij}(\mathbf{r}) \qquad \text{(Equation 3)}$$

We note that the electronic population term ρ_{ii} is time-independent in the absence of non-adiabatic transitions between different electronic states. The time-dependence of the total charge density is thus contributed solely by the purely electronic coherence term $\sigma^{\mathrm{E}}_{\mathrm{coh}}(\mathbf{r},t)$ in Equation 3, which is responsible for the time-evolving electron dynamics in molecules.

The theoretical description of the time-resolved diffraction signal in this article is based on the off-resonant single-molecule (gas-phase) time-resolved X-ray/electron diffraction in the minimal coupling picture.[40,43]The time-resolved single-molecule diffraction signal is given by[44]

$$S(\mathbf{q},T) \propto W_0(\Delta\omega)\int dt|\mathbf{A}_\mathbf{X}(t-T)|^2\tilde{S}(\mathbf{q},t) \quad \text{(Equation 4)}$$

where $\mathbf{A}_\mathbf{X}(t-T)$ is the X-ray/electron probe pulse vector potential at delay time T from the pump pulse, $\mathbf{q}$ is the scattering momentum transfer, $W_0(\Delta\omega)$ is a window function for a frequency detection widow $\Delta\omega$ and $\tilde{S}(\mathbf{q},t)$ is the time-dependent molecular response in X-ray/electron diffraction.[42,45,46] We assume a window function much broader than the relevant electronic transition energies of the system so that $W_0(\Delta\omega)$ is independent of the molecular response.

The time-resolved molecular response in X-ray diffraction, $\tilde{S}(\mathbf{q},t)$, in Equation 4 is given by

$$\tilde{S}^{\mathrm{XRD}}(\mathbf{q},t) = \sum_{ijk}\rho_{ji}(t)\left\langle\chi_i(t)\middle|\hat{\sigma}^{\mathrm{E}}_{ik}(-\mathbf{q})\hat{\sigma}^{\mathrm{E}}_{kj}(\mathbf{q})\middle|\chi_j(t)\right\rangle \quad \text{(Equation 5)}$$

where $\hat{\sigma}^{\mathrm{E}}_{kj}(\mathbf{q})$ is the electronic charge-density operator in momentum-space. Similar to the Equation 2, the time-resolved X-ray diffraction signal can be partitioned into the sum of contributions from electronic populations $\tilde{S}^{\mathrm{XRD}}_{\mathrm{pop}}(\mathbf{q},t)$ and coherences $\tilde{S}^{\mathrm{XRD}}_{\mathrm{coh}}(\mathbf{q},t)$,

$$\tilde{S}^{\mathrm{XRD}}(\mathbf{q},t) = \tilde{S}^{\mathrm{XRD}}_{\mathrm{pop}}(\mathbf{q},t) + \tilde{S}^{\mathrm{XRD}}_{\mathrm{coh}}(\mathbf{q},t) \quad \text{(Equation 6)}$$

where

$$\tilde{S}^{\mathrm{XRD}}_{\mathrm{pop}}(\mathbf{q},t) = \sum_i\rho_{ii}(t)\sum_k\langle\chi_i(t)|\hat{\sigma}^{\mathrm{E}}_{ik}(-\mathbf{q})\hat{\sigma}^{\mathrm{E}}_{ki}(\mathbf{q})|\chi_i(t)\rangle \quad \text{(Equation 7)}$$

$$\tilde{S}^{\mathrm{XRD}}_{\mathrm{coh}}(\mathbf{q},t) = 2\Re\left[\sum_{j>i}\rho_{ji}(t)\sum_k\left\langle\chi_i(t)\middle|\hat{\sigma}^{\mathrm{E}}_{ik}(-\mathbf{q})\hat{\sigma}^{\mathrm{E}}_{kj}(\mathbf{q})\middle|\chi_j(t)\right\rangle\right] \quad \text{(Equation 8)}$$

Unlike X-ray scattering, which is dominated by the molecular electronic charge density, electron scattering originates from the electrostatic Coulomb interaction of the incoming electrons with both molecular electrons and nuclei. The interaction between charged particles resulting a $1/q^4$ term in the Rutherford scattering.[47] The time-resolved molecular response in Equation 4 becomes $\tilde{S}(\mathbf{q},t) = \frac{1}{q^4}\tilde{S}^{\mathrm{UED}}(\mathbf{q},t)$ where $\tilde{S}^{\mathrm{UED}}(\mathbf{q},t)$ is given by

$$\begin{aligned}\tilde{S}^{\mathrm{UED}}(\mathbf{q},t) &= \sum_{ijk}\rho_{ji}(t)\left\langle\chi_i(t)\middle|\hat{\sigma}^{\mathrm{E}}_{ik}(-\mathbf{q})\hat{\sigma}^{\mathrm{E}}_{kj}(\mathbf{q})\middle|\chi_j(t)\right\rangle + \sum_i\rho_{ii}(t)\langle\chi_i(t)|\hat{\sigma}^{\mathrm{N}}_{ii}(-\mathbf{q})\hat{\sigma}^{\mathrm{N}}_{ii}(\mathbf{q})|\chi_j(t)\rangle \\ &\quad + 2\Re\left[\sum_{ij}\rho_{ji}(t)\langle\chi_i(t)\middle|\hat{\sigma}^{\mathrm{E}}_{ij}(-\mathbf{q})\hat{\sigma}^{\mathrm{N}}_{jj}(\mathbf{q})\middle|\chi_j(t)\rangle\right] \\ &= \tilde{S}^{\mathrm{UED}}_{\mathrm{elec}}(\mathbf{q},t) + \tilde{S}^{\mathrm{UED}}_{\mathrm{nucl}}(\mathbf{q},t) + \tilde{S}^{\mathrm{UED}}_{\mathrm{mixed}}(\mathbf{q},t) \quad \text{(Equation 9)}\end{aligned}$$

Here $\hat{\sigma}^{\mathrm{N}}_{ii}(\mathbf{q})$ is the nuclear charge-density operator in momentum-space, $\tilde{S}^{\mathrm{UED}}_{\mathrm{elec}}(\mathbf{q},t)$ is the electronic contribution to the signal which is identical to $\tilde{S}^{\mathrm{XRD}}(\mathbf{q},t)$ given by Equation 5. In addition to the electronic contribution, $\tilde{S}^{\mathrm{UED}}_{\mathrm{nucl}}(\mathbf{q},t)$ is the nuclear contribution to the signal and $\tilde{S}^{\mathrm{UED}}_{\mathrm{mixed}}(\mathbf{q},t)$ is the mixed electronic-nuclear interference in electron diffraction which are distinct from X-ray diffraction as illustrated in Figure 1.

RECENT ADVANCES IN ULTRAFAST GAS-PHASE DIFFRACTION EXPERIMENTS

Ultrafast gas-phase diffraction experiments, including X-ray scattering and electron diffraction, have undergone significant advancements in recent years. These experiments typically employ a pump-probe scheme (see Figure 2), where a pump pulse excites the molecule to a higher electronic state, followed by a delayed probe pulse (either X-ray or electron beam) that interacts with the excited molecule. By varying the time delay between the pump and probe pulses, the structural evolution of the molecule can be followed in real-time.

The advent of XFELs, with their ultrashort pulse durations and extreme brightness,[48,49] has revolutionized ultrafast X-ray scattering for studying structural dynamics in free molecules. Proof-of-principle femtosecond gas-phase X-ray scattering experiments conducted at Linac Coherent Light Source[50,51] resulted in a "molecular movie" of the ring-opening reaction of 1,3-cyclohexadiene.[52] Subsequent improvements, such as a newly designed diffractometer, shot-to-shot X-ray intensity fluctuation calibration, generalized detector geometry calibration, and various data processing advancements,[53,54] have enhanced signal-to-noise ratios and enabled detailed studies of molecules and chemical dynamics in excited states. These studies include the investigation of ultrafast nuclear motions during chemical reactions,[55–58] the determination of polyatomic molecular structures in electronically excited states,[59] the observation of bond elongation and contraction during charge transfer,[60] and the direct measurement of the redistribution of molecular electron density immediately after photoexcitation.[61] Further examples include studies of chemical kinetics,[62,63] anharmonicities, and correlations.[64]

Concurrently, gas-phase MeV-UED has emerged as another powerful tool for probing structural dynamics in isolated molecules. Pioneering MeV-UED studies at SLAC National Accelerator Laboratory demonstrated the capability of imaging vibrational wavepacket motion in I_2 with sub-angstrom spatial and 230 fs time resolution, confirming MeV-UED's potential for tracking atomic motion in gas-phase molecules.[65] Since then, MeV-UED has been extended to study reaction dynamics in more complex molecules, such as imaging the nonadiabatic dynamics of CF_3I,[66] observing the isomerization of hexatriene following the photoinduced ring-opening of 1,3-cyclohexadiene,[67] capturing the

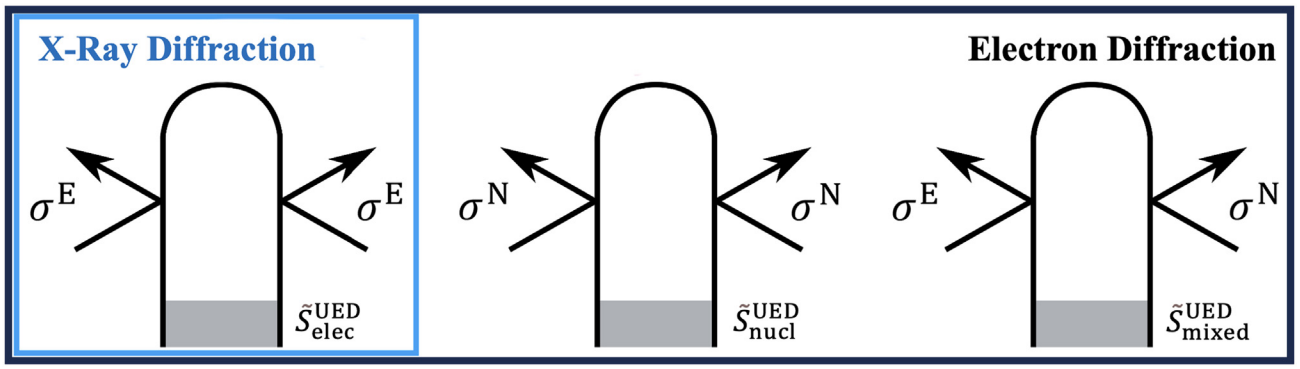

Figure 1. Loop diagrams for single-molecule time-resolved X-ray diffraction (blue box) and electron diffraction (black box)

"pericyclic minimum" intermediate in α-terpinene,[68] and revealing competing dissociation channels in CS_2.[69] Furthermore, MeV-UED has demonstrated the ability to simultaneously record both nuclear and electronic dynamics by exploiting inelastic scattering signals, as shown in studies of pyridine and ammonia molecules.[70,71]

FUTURE PERSPECTIVES: TRACKING QUANTUM COHERENCES IN MOLECULES

Recent advancements in both X-ray scattering and electron diffraction have established ultrafast gas-phase scattering as powerful tools for observing structural dynamics originated from vibrational coherences on femtosecond timescales and sub-angstrom length scales. The ongoing development of attosecond X-ray free electron lasers and electron sources promises to open new frontiers in the study of ultrafast molecular dynamics. By pushing the temporal resolution to the attosecond regime, these techniques could enable the direct observation of attosecond electron dynamics and vibronic coupling in molecules.

Probing attosecond electron dynamics driven by electronic coherences

The interaction between a molecule and a broadband light source can lead to the creation of a superposition of electronic states, causing time-dependent variations in the molecule's charge density. This phenomenon, referred to as charge migration, occurs on attosecond timescales and is solely a result of electronic coherence. Real-time experimental observation of charge migration is vital for optimizing and controlling fundamental events in various chemical and biophysical processes and has been a primary focus of attosecond molecular science.[72–74] However, directly observing the time-evolving charge density in real space remains a significant challenge. As shown in Theory section, ultrafast X-ray and electron diffraction techniques have the potential to directly capture the spatiotemporal evolution of a molecule's electronic charge density. Several recent theoretical studies have investigated the use of ultrafast X-ray scattering to probe charge migration.[46,75–77] With the ongoing development of attosecond hard XFELs worldwide,[25,26] experimental realizations of attosecond X-ray diffraction are expected in the near future. Attosecond electron diffraction, although technically more challenging due to the space-charge effect, has shown

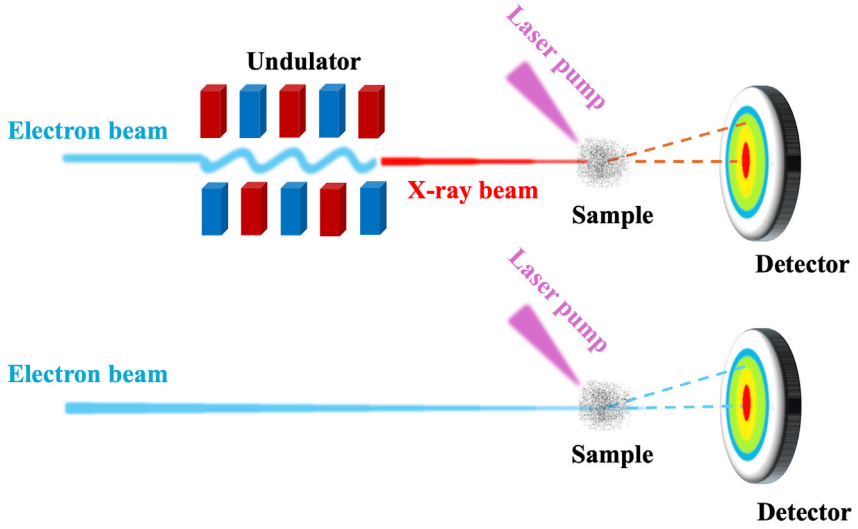

Figure 2. Experimental set-ups for ultrafast gas-phase X-ray (top) and electron diffraction (bottom)

promise for gas-phase implementation thanks to recent advancements in attosecond electron pulse generation and single-electron pulse techniques.[28,29]

As evident from Equations 5 and 9, ultrafast X-ray and electron diffraction can track charge migration, but the molecular charge density in real space (Equation 3) cannot be directly obtained from these signals as they measure the expectation values of products of charge-density operators. A recent theoretical work proposed a novel experimental scheme which combines ultrafast X-ray and electron diffraction techniques.[46] This approach has the potential to overcome the aforementioned limitation and enable real-space imaging of attosecond electron dynamics in isolated molecules. This is achieved by isolating the mixed contribution, $\tilde{S}^{\mathrm{UED}}_{\mathrm{mixed}}$ in Equation 9.

By carefully normalizing and subtracting the ultrafast X-ray (Equation 5) and electron diffraction (Equation 9) signals, one obtains $S^{\mathrm{diff}}(\mathbf{q},t) = \tilde{S}^{\mathrm{UED}}_{\mathrm{nucl}}(\mathbf{q},t) + \tilde{S}^{\mathrm{UED}}_{\mathrm{mixed}}(\mathbf{q},t)$. In the charge migration regime, where nuclear motions are negligible, $\tilde{S}^{\mathrm{UED}}_{\mathrm{nucl}}(\mathbf{q},t)$ is time-independent. The time-dependent difference signal is then given by $\Delta S^{\mathrm{diff}}(\mathbf{q},t) = \Delta\tilde{S}^{\mathrm{UED}}_{\mathrm{mixec}}(\mathbf{q},t) = 2\Re[\Delta\sigma^{\mathrm{E}}_{\mathrm{tot}}(-\mathbf{q},t)\sigma^{\mathrm{N}}_{0}(\mathbf{q})]$ where $\Delta\sigma^{\mathrm{E}}_{\mathrm{tot}}(\mathbf{q},t) = \sigma^{\mathrm{E}}_{\mathrm{tot}}(\mathbf{q},t) - \sigma^{\mathrm{E}}_{0}(\mathbf{q})$ is the difference electronic charge density in q-space, and $\sigma^{\mathrm{E}}_{0}(\mathbf{q})$ is the total electronic charge density prior to the pump pulse (i.e., $\sigma^{\mathrm{E}}_{\mathrm{tot}}(\mathbf{q},t<0)$). The time-dependent difference signal $\Delta S^{\mathrm{diff}}(\mathbf{q},t)$ is solely contributed by the mixed nuclear-electronic term $\Delta\tilde{S}^{\mathrm{UED}}_{\mathrm{mixed}}$. Since the molecular nuclei remain stationary during the attosecond charge migration dynamics, the resulting time-dependent difference signal forms an interference between the $\sigma^{\mathrm{E}}_{\mathrm{tot}}(\mathbf{q},t)$ and the $\sigma^{\mathrm{N}}_{0}(\mathbf{q})$. $\sigma^{\mathrm{N}}_{0}(\mathbf{q})$ serves as a static reference local oscillator. This generates a heterodyne signal without the need for an additional field, enabling direct measurement of the time-evolving electronic charge density $\sigma^{\mathrm{E}}_{\mathrm{tot}}(\mathbf{q},t)$. As the time-dependence of $\sigma^{\mathrm{E}}_{\mathrm{tot}}(\mathbf{q},t)$ in Equation 3 originates from its electronic coherence contribution (i.e., $\sigma^{\mathrm{E}}_{\mathrm{coh}}(\mathbf{r},t)$), this provides spatial resolution of electron motions induced by purely electronic coherence. The ground-state nuclear geometry is assumed to be known *a priori*, obtainable through static diffraction measurements or high-level quantum chemistry calculations. Accurate determination of the ground-state nuclear geometry is crucial, as it can affect the accuracy of the reconstructed $\Delta\sigma^{\mathrm{E}}_{\mathrm{tot}}(\mathbf{q},t)$. This approach allows for the inversion of the signal from momentum space to real space, generating a "molecular movie" of attosecond charge migration. This concept has been demonstrated through theoretical simulations to image the fast charge oscillation dynamics within a benzene ring of a fluorinated biphenyl molecule in real space (see Figure 3). We note that while this technique is applicable to randomly oriented samples, a high degree of alignment is desired in order to retrieve the full three-dimensional electronic charge densities rather than its one-dimensional radial distribution from an isotropic sample.

One of the main challenges for implementing such an experiment is the non-trivial data analysis procedure required when subtracting two diffraction signals. Note that because X-ray diffraction is proportional to the Thomson cross section while electron diffraction is proportional to the Rutherford cross section, careful normalization is required when combining two individual measurements. This is crucial for isolating the desired mixed contribution to the signal. One possible solution is to normalize the individual diffraction signals using their intrinsic properties when $\mathbf{q}\rightarrow 0$. It is known that the $\tilde{S}^{\mathrm{XRD}}$ in Equation 5 is proportional to the square of the total number of electrons (N^2_{el}) in the molecule when $\mathbf{q}\rightarrow 0$, while the $\tilde{S}^{\mathrm{UED}}$ vanishes when $\mathbf{q}\rightarrow 0$ due to the opposite charges of electrons and nuclei canceling out.[78] In addition, the diffraction signals should be deconvoluted with their respective instrument functions in the subtraction procedure to avoid errors coming from pulse-length deviations.

Probing vibronic coherences at conical intersections

Conical intersections (CIs) are important regions where two or more adiabatic potential energy surfaces become degenerate, resulting in strong non-adiabatic couplings between them. Because these regions allow for efficient, non-radiative electronic relaxations, they play critical roles in virtually all photochemical and photophysical processes. Conventional experimental signatures of CIs are primarily based on the transfer of electronic populations between electronic states. Directly observing the passage through CIs via transient vibronic coherences remains challenging, as many contemporary ultrafast measurements are dominated by much stronger signals from electronic populations that are not specific to CIs.

As manifested in Equation 8, time-resolved X-ray diffraction contains a mixed elastic-inelastic scattering term $\tilde{S}^{\mathrm{XRD}}_{\mathrm{coh}}(\mathbf{q},t)$ originating from vibronic coherences. However, this mixed coherence term is found to be significantly weaker than the dominating contributions from electronic populations $\tilde{S}^{\mathrm{XRD}}_{\mathrm{pop}}(\mathbf{q},t)$ during CI passage, making its experimental realization very challenging. A recent theoretical article has shown that this major obstacle in standard ultrafast X-ray diffraction can be overcome by measuring the rotationally averaged time-resolved X-ray diffraction using twisted X-ray beams carrying orbital angular momentum (OAM).[79] Twisted beams, also known as vortex or OAM beams, possess a helical spatial wavefront that twists along the beam propagation direction, as shown in Figure 4A, independently of the beam polarization state. Various strategies have been developed to generate intense, hard X-ray twisted beams,[80–82] enabling ultrafast spectroscopic measurements of molecules using these OAM beams.[83] Twisted X-ray scattering provides structural information in addition to energy observables in molecules, showing promise in revealing both the spatial and temporal profiles of transient vibronic coherences generated at CIs.

The vector potential $\mathbf{A}_{\mathrm{X}}$ of OAM beams is given by

$$\mathbf{A}_{\mathrm{X}}(\mathbf{r},t) = E(t)A_l(r,z,\phi) = E(t)A(r,z)e^{il\phi} \qquad \text{(Equation 10)}$$

where $A(r,z)$ is the radial profile of the beam at height z and $E(t)$ is the temporal profile. Over the molecular scale, the radial profile $A(r,z)$ can be assumed as a constant. The angular index l is called the topological charge of the twisted beam. Twisted beams are eigenstates of the angular momentum operator, and possess an orbital angular momentum (OAM) of $l\hbar$ per photon. Here the beam profile is expressed in cylindrical coordinates, where r is the radial distance, ϕ is angular coordinate and z is axial coordinate. The OAM beam polarization can be kept

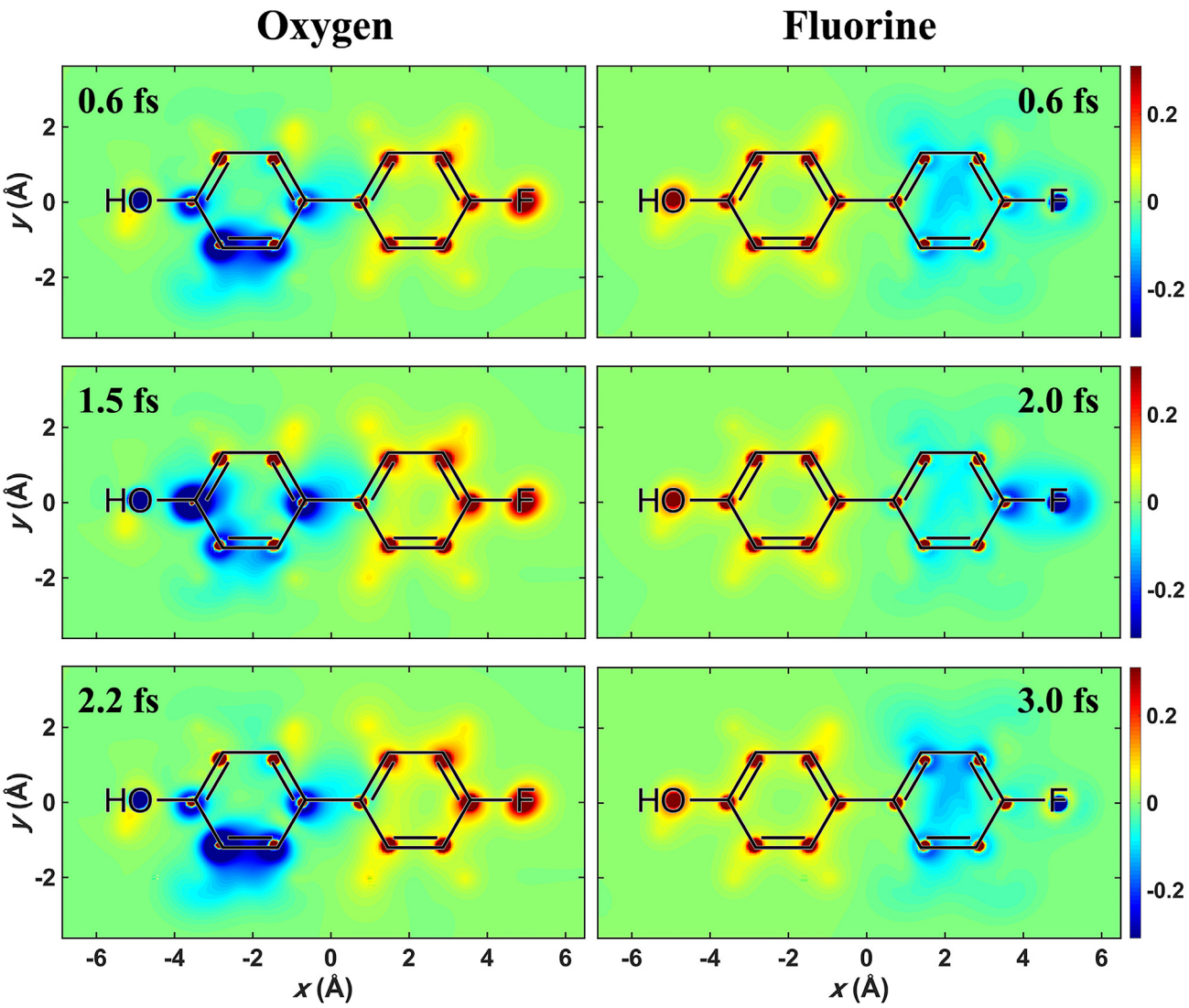

Figure 3. Snapshots of the difference in electronic charge density, $\Delta\sigma^{E}_{tot}(\mathbf{r},t)$, in real space for the 4-fluoro-4′-hydroxybiphenyl following oxygen K-edge (left) and fluorine K-edge (right) excitations

Reprinted with permission from ref. 46. Copyright 2022 by the American Chemistry Society.

linear in the proposed setup and gets absorbed in a Lorentz-polarization factor $|\epsilon_x \cdot \epsilon_s|^2$ in Equation 4, where ϵ_x and ϵ_s are polarization vectors of the X-ray probe pulse and scattered photon.

The time-resolved twisted X-ray diffraction signal is obtained by substituting Equation 10 in Equations 4 and 5,[79]

$$S_l(\mathbf{q},T) \propto \int dt |E(t-T)|^2 \tilde{S}_l(\mathbf{q},t) \qquad \text{(Equation 11)}$$

where $\tilde{S}_l(\mathbf{q},t) = \langle \hat{\sigma}_l^{\dagger}(\mathbf{q},t)\hat{\sigma}_l(\mathbf{q},t)\rangle$ and $\hat{\sigma}_l(\mathbf{q}) = \int \hat{\sigma}^{E}(\mathbf{r}) e^{il\phi} e^{i\mathbf{q}\cdot\mathbf{r}} d\mathbf{r}$ is the momentum-space electronic charge-density operator carrying OAM. Similar to the Equations 6, 7, and 8, the time-resolved twisted X-ray diffraction signal can be partitioned into the sum of contributions from electronic populations and coherences,

$$\tilde{S}_l(\mathbf{q},t) = \tilde{S}_l^{pop}(\mathbf{q},t) + \tilde{S}_l^{coh}(\mathbf{q},t) \qquad \text{(Equation 12)}$$

The full derivation of the signal has been discussed previously.[79] It has been shown that when taking the difference of the rotationally averaged diffraction signal measured with the positive and negative OAM beams, i.e., $\Delta S_l(q,T) = \langle S_l(\mathbf{q},T)\rangle_\Omega - \langle S_{-l}(\mathbf{q},T)\rangle_\Omega$, the contributions of electronic populations, $\tilde{S}_l^{pop}(\mathbf{q},t)$, cancel out and only the desired coherence signal, $\tilde{S}_l^{coh}(\mathbf{q},t)$, survive. Here q is the norm of the momentum transfer vector $\mathbf{q}$ and $\langle \ldots \rangle_\Omega$ denotes the rotationally averaged diffraction signal.

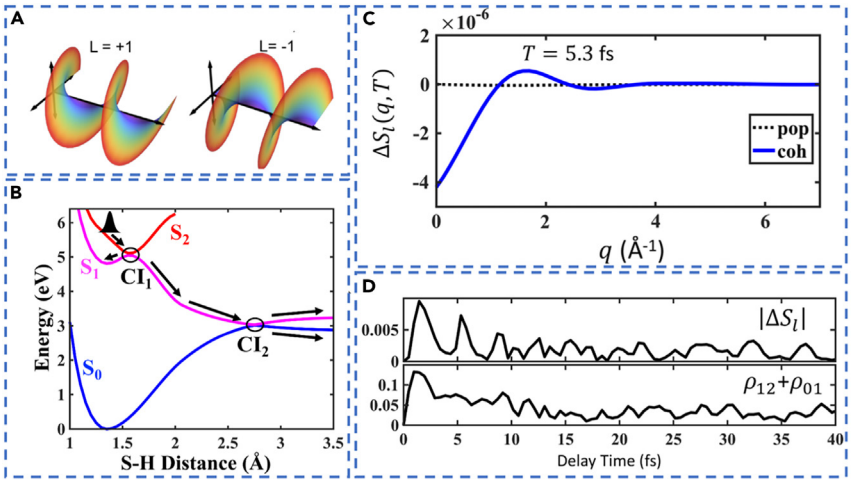

Figure 4. Illustrations and simulations of twisted X-ray scattering

(A) Helical spatial wavefronts of twisted beams carrying various OAMs (L = +1 and L = −1).

(B) Reaction pathway of thiophenol S-H photodissociation. Two CIs are marked with open circles.

(C) The difference of simulated rotationally averaged diffraction signals, $\Delta S_l(q,T)$, of thiophenol at 5.3 fs delay time for population and coherence contribution, respectively.

(D) Comparison of the simulated signal, $\Delta S_l(q,T)$, integrated over q and the total coherence magnitude of the vibronic coherences at two CIs of thiophenol photodissociation calculated by quantum dynamics. Adapted with permission from ref. 79. Copyright 2022 by the American Physical Society.

Previous simulation has demonstrated the concept by applying it to thiophenol photodissociation shown in Figure 4B involving two CIs (S_2/S_1 and S_1/S_0 CI) calculated by exact quantum dynamical simulations.[79] The simulated quantum dynamics was used to simulate the time-resolved rotationally averaged diffraction signals, $S_l(q,T)$ for $l = 1$ and $l = -1$ OAM X-ray beams. Figure 4C shows their difference signal at a chosen delay time which demonstrates that the population contribution to the isotropic difference signal $\Delta S_l^{\mathrm{pop}}(q,T)$ vanishes so that only coherence signal contributes to the total difference signal $\Delta S_l(q,T)$. The time-resolved difference signal, $\Delta S_l(q,T)$, was further simulated for the entire thiophenol photodissociation dynamics. Figure 4D shows the time-dependent absolute difference signal integrated over q. For comparison, the sum of the S_2/S_1 and S_1/S_0 vibronic coherence magnitudes given by the quantum dynamical simulations is also shown. The integrated difference signal clearly resembles the time-dependent vibronic coherences in the molecule. By implementing this difference measurement scheme, one could potentially directly monitor the passage through CIs imprinted in the transient vibronic coherences.

A major challenge is the inevitably weak magnitude of the coherence signal. The signal shown in Figure 4C is about three orders of magnitude smaller than the detection limit reported so far in existing ultrafast gas-phase X-ray diffraction experiments.[14] These experiments were performed at XFEL facilities with a repetition rate of 120 Hz. To achieve a high signal-to-noise ratio for resolving the desired electronic coherence signal, the ongoing development of high-repetition-rate (MHz) hard X-ray sources is beneficial for the realization of the proposed experiment. Alternatively, employing a weak resonant infrared field to enhance coherence signatures in diffraction signals could be helpful.[84]

It is worth pointing out that since the proposed technique essentially relies solely on the coherence contribution to the diffraction signal (i.e., $\tilde{S}_{\mathrm{coh}}^{\mathrm{XRD}}$ in Equation 8), its application is more general, going beyond vibronic coherences at CIs. It can be applied to spatially resolve many other fundamental quantum coherence phenomena in molecules, including attosecond charge migration discussed in probing attosecond electron dynamics driven by electronic coherences.

CONCLUSION

Ultrafast gas-phase X-ray scattering and electron diffraction have proven to be powerful tools for investigating the nuclear dynamics of molecules with atomic spatial and temporal resolution. Recent theoretical developments, including the use of twisted X-ray beams and the combination of X-ray and electron diffraction techniques, unveiled the potential to extend these methods into the attosecond domain. This would allow for the direct observation of electronic and vibronic coherences that play critical roles in photochemical processes. By resolving charge migration in real-space and time, and disentangling the intricate coupling between electronic and nuclear degrees of freedom at conical intersections, these emerging techniques will provide valuable insights into the fundamental mechanisms underlying chemical reactivity. As attosecond X-ray and electron sources continue to advance, we expect these tools to open new avenues for exploring the quantum dynamics of molecules at their most fundamental level.

To fully harness the potential of ultrafast gas-phase diffraction, continued advancements in instrumentation, theoretical modeling, and data analysis are necessary. Overcoming the challenges associated with generating intense and stable attosecond pulses, improving detector performance, and developing robust data inversion algorithms will require a concerted effort from the scientific community. By addressing these limitations, we anticipate that ultrafast gas-phase diffraction will provide unprecedented insights into the quantum dynamics of

molecules, ultimately paving the way for the rational design and control of chemical reactions at the attosecond scale. This will not only deepen our understanding of the fundamental principles governing chemical reactivity but also have far-reaching implications for fields such as photocatalysis, energy conversion, and quantum technologies.

LIMITATIONS OF THE STUDY

This article reflects the authors' perspective on the current state and future potential of ultrafast gas-phase X-ray scattering and electron diffraction techniques. It is important to acknowledge that challenges remain in the development and application of these methods. Generating sufficiently intense and stable attosecond pulses, improving detector performance, and developing robust data inversion algorithms will require a concerted effort from the scientific community. Addressing these limitations will be crucial for realizing the full potential of ultrafast gas-phase diffraction in unraveling the quantum dynamics of molecules at the attosecond scale.

ACKNOWLEDGMENTS

This research was supported in part by W. M. Keck Foundation through computing resources at the W. M. Keck Laboratory for Integrated Biology at UC San Diego.

AUTHOR CONTRIBUTIONS

Conceptualization, Z.T. and H.Y.; investigation, Z.T., R.J. and H.Y.; writing – original draft, Z.T. and H.Y.; writing – review and editing, Z.T., R.J. and H.Y.; and supervision, H.Y.

DECLARATION OF INTERESTS

The authors declare no competing interests.

REFERENCES

1. Tannor, D.J., Kosloff, R., and Rice, S.A. (1986). Coherent pulse sequence induced control of selectivity of reactions: Exact quantum mechanical calculations. J. Chem. Phys. *85*, 5805–5820.
2. Zewail, A.H. (2000). Femtochemistry: Atomic-scale dynamics of the chemical bond. J. Phys. Chem. A *104*, 5660–5694.
3. Scholes, G.D., Fleming, G.R., Chen, L.X., Aspuru-Guzik, A., Buchleitner, A., Coker, D.F., Engel, G.S., van Grondelle, R., Ishizaki, A., Jonas, D.M., et al. (2017). Using coherence to enhance function in chemical and biophysical systems. Nature *543*, 647–656.
4. Cao, J., Cogdell, R.J., Coker, D.F., Duan, H.G., Hauer, J., Kleinekathöfer, U., Jansen, T.L.C., Mančal, T., Miller, R.J.D., Ogilvie, J.P., et al. (2020). Quantum biology revisited. Sci. Adv. *6*, eaaz4888.
5. Wasielewski, M.R., Forbes, M.D.E., Frank, N.L., Kowalski, K., Scholes, G.D., Yuen-Zhou, J., Baldo, M.A., Freedman, D.E., Goldsmith, R.H., Goodson, T., 3rd, et al. (2020). Exploiting chemistry and molecular systems for quantum information science. Nat. Rev. Chem *4*, 490–504.
6. Williamson, J.C., Cao, J., Ihee, H., Frey, H., and Zewail, A.H. (1997). Clocking transient chemical changes by ultrafast electron diffraction. Nature *386*, 159–162.
7. King, W.E., Campbell, G.H., Frank, A., Reed, B., Schmerge, J.F., Siwick, B.J., Stuart, B.C., and Weber, P.M. (2005). Ultrafast Electron Microscopy in Materials Science, Biology, and Chemistry. J. Appl. Phys. *36*, 111101–111127.
8. Gaffney, K.J., and Chapman, H.N. (2007). Imaging atomic structure and dynamics with ultrafast x-ray scattering. Science *316*, 1444–1448.
9. Sciaini, G., and Miller, R.J.D. (2011). Femtosecond electron diffraction: heralding the era of atomically resolved dynamics. Rep. Prog. Phys. *74*, 096101.
10. Ischenko, A.A., Weber, P.M., and Miller, R.J.D. (2017). Capturing Chemistry in Action with Electrons: Realization of Atomically Resolved Reaction Dynamics. Chem. Rev. *117*, 11066–11124.
11. Ihee, H., Lobastov, V.A., Gomez, U.M., Goodson, B.M., Srinivasan, R., Ruan, C.Y., and Zewail, A.H. (2001). Direct Imaging of Transient Molecular Structures with Ultrafast Diffraction. Science *291*, 458–462.
12. Ruan, C.Y., Lobastov, V.A., Srinivasan, R., Goodson, B.M., Ihee, H., and Zewail, A.H. (2001). Ultrafast diffraction and structural dynamics: The nature of complex molecules far from equilibrium. Proc. Natl. Acad. Sci. USA *98*, 7117–7122.
13. Dudek, R.C., and Weber, P.M. (2001). Ultrafast Diffraction Imaging of the Electrocyclic Ring-Opening. J. Phys. Chem. *105*, 4167–4171.
14. Yong, H., Kirrander, A., and Weber, P.M. (2023). Time-resolved x-ray scattering of excited state structure and dynamics in Structural Dynamics with X-ray and Electron Scattering. Royal Society of Chemistry *25*, 344–373.
15. Centurion, M., Wolf, T.J.A., and Yang, J. (2022). Ultrafast imaging of molecules with electron diffraction. Annu. Rev. Phys. Chem. *73*, 21–42.
16. Odate, A., Kirrander, A., Weber, P.M., and Minitti, M.P. (2023). Brighter, faster, stronger: ultrafast scattering of free molecules. Adv. Phys. X *8*, 2126796.
17. Lee, Y., Oang, K.Y., Kim, D., and Ihee, H. (2024). A comparative review of time-resolved x-ray and electron scattering to probe structural dynamics. Struct. Dyn. *11*, 031301.
18. Wang, Q., Yun, L., and Yang, J. (2024). Ultrafast Molecular Movies: Probing Chemical Dynamics with Femtosecond Electron and X-Ray Diffraction. CCS Chem. *6*, 1092–1109.
19. Goulielmakis, E., Loh, Z.H., Wirth, A., Santra, R., Rohringer, N., Yakovlev, V.S., Zherebtsov, S., Pfeifer, T., Azzeer, A.M., Kling, M.F., et al. (2010). Real-time observation of valence electron motion. Nature *466*, 739–743.
20. Calegari, F., Ayuso, D., Trabattoni, A., Belshaw, L., De Camillis, S., Anumula, S., Frassetto, F., Poletto, L., Palacios, A., Decleva, P., et al. (2014). Ultrafast electron dynamics in phenylalanine initiated by attosecond pulses. Science *346*, 336–339.
21. Kraus, P.M., Mignolet, B., Baykusheva, D., Rupenyan, A., Horný, L., Penka, E.F., Grassi, G., Tolstikhin, O.I., Schneider, J., Jensen, F., et al. (2015). Measurement and laser control of attosecond charge migration in ionized iodoacetylene. Science *350*, 790–795.
22. Månsson, E.P., Latini, S., Covito, F., Wanie, V., Galli, M., Perfetto, E., Stefanucci, G., Hübener, H., De Giovannini, U., Castrovilli, M.C., et al. (2021). Real-time observation of a correlation-driven sub 3 fs charge migration in ionized adenine. Commun. Chem. *4*, 73.
23. Barillot, T., Alexander, O., Cooper, B., Driver, T., Garratt, D., Li, S., Al Haddad, A., Sanchez-Gonzalez, A., Agåker, M., Arrell, C., et al. (2021). Correlation-driven transient hole dynamics resolved in space and time in the isopropanol molecule. Phys. Rev. X *11*, 031048.
24. Li, S., Driver, T., Rosenberger, P., Champenois, E.G., Duris, J., Al-Haddad, A., Averbukh, V., Barnard, J.C.T., Berrah, N., Bostedt, C., et al. (2022). Attosecond coherent electron motion in Auger-Meitner decay. Science *375*, 285–290.
25. Duris, J., Li, S., Driver, T., Champenois, E.G., MacArthur, J.P., Lutman, A.A., Zhang, Z., Rosenberger, P., Aldrich, J.W., Coffee, R., et al. (2020). Tunable isolated attosecond x-ray pulses with gigawatt peak power from a free-electron laser. Nat. Photonics *14*, 30–36.
26. Xiao, Y., Feng, C., and Liu, B. (2022). Generating isolated attosecond x-ray pulses

by wavefront control in a seeded free-electron laser. Ultrafast Sci. *2022*, 9812478.
27. Franz, P., Li, S., Driver, T., Robles, R., Cesar, D., Isele, E., Guo, Z., Wang, J., Duris, J., Larsen, K., et al. (2024). Terawatt-scale attosecond X-ray pulses from a cascaded superradiant free-electron laser. Nat. Photon *18*, 698–703.
28. Baum, P. (2013). On the physics of ultrashort single-electron pulses for time-resolved microscopy and diffraction. Chem. Phys. *423*, 55–61.
29. Morimoto, Y., and Baum, P. (2018). Diffraction and microscopy with attosecond electron pulse trains. Nat. Phys. *14*, 252–256.
30. Merritt, I.C.D., Jacquemin, D., and Vacher, M. (2021). Attochemistry: Is controlling electrons the future of photochemistry? J. Phys. Chem. Lett. *12*, 8404–8415.
31. Calegari, F., and Martin, F. (2023). Open questions in attochemistry. Commun. Chem. *6*, 184.
32. Scholes, G.D., Fleming, G.R., Olaya-Castro, A., and van Grondelle, R. (2011). Lessons from nature about solar light harvesting. Nat. Chem. *3*, 763–774.
33. Brieke, C., Rohrbach, F., Gottschalk, A., Mayer, G., and Heckel, A. (2012). Light-Controlled Tools. Angew. Chem. Int. Ed. *51*, 8446–8476.
34. Szymański, W., Beierle, J.M., Kistemaker, H.A.V., Velema, W.A., and Feringa, B.L. (2013). Reversible photocontrol of biological systems by the incorporation of molecular photoswitches. Chem. Rev. *113*, 6114–6178.
35. Ben-Nun, M., Martínez, T.J., Weber, P.M., and Wilson, K.R. (1996). Direct Imaging of Excited Electronic States Using Diffraction Techniques: Theoretical Considerations. Chem. Phys. Lett. *263*, 405–414.
36. Ben-Nun, M., Cao, J., and Wilson, K.R. (1997). Ultrafast X-Ray and Electron Diffraction: Theoretical Considerations. J. Phys. Chem. A *101*, 8743–8761.
37. Cao, J., and Wilson, K.R. (1998). Ultrafast X-Ray Diffraction Theory. J. Phys. Chem. A *102*, 9523–9530.
38. Henriksen, N.E., and Møller, K.B. (2008). On the Theory of Time-Resolved X-Ray Diffraction. J. Phys. Chem. B *112*, 558–567.
39. Dixit, G., Vendrell, O., and Santra, R. (2012). Imaging Electronic Quantum Motion with Light. Proc. Natl. Acad. Sci. USA *109*, 11636–11640.
40. Bennett, K., Kowalewski, M., Rouxel, J.R., and Mukamel, S. (2018). Monitoring Molecular Nonadiabatic Dynamics with Femtosecond X-Ray Diffraction. Proc. Natl. Acad. Sci. USA *115*, 6538–6547.
41. Simmermacher, M., Henriksen, N.E., Møller, K.B., Moreno Carrascosa, A., and Kirrander, A. (2019). Electronic Coherence in Ultrafast X-Ray Scattering from Molecular Wave Packets. Phys. Rev. Lett. *122*, 073003.
42. Simmermacher, M., Moreno Carrascosa, A., E Henriksen, N., B Møller, K., and Kirrander, A. (2019). Theory of Ultrafast X-Ray Scattering by Molecules in the Gas Phase. J. Chem. Phys. *151*, 174302.
43. Rouxel, J.R., Keefer, D., and Mukamel, S. (2021). Signatures of electronic and nuclear coherences in ultrafast molecular x-ray and electron diffraction. Struct. Dyn. *8*, 014101.
44. Yong, H., Keefer, D., and Mukamel, S. (2023). Novel Ultrafast Molecular Imaging Based on the Combination of X-ray and Electron Diffraction. J. Phys. Chem. A *127*, 835–841.
45. Dixit, G., Slowik, J.M., and Santra, R. (2014). Theory of time-resolved nonresonant x-ray scattering for imaging ultrafast coherent electron motion. Phys. Rev. *89*, 043409.
46. Yong, H., Sun, S., Gu, B., and Mukamel, S. (2022). Attosecond charge migration in molecules imaged by combined x-ray and electron diffraction. J. Am. Chem. Soc. *144*, 20710–20716.
47. Brockway, L.O. (1936). Electron Diffraction by Gas Molecules. Rev. Mod. Phys. *8*, 231–266.
48. Emma, P., Akre, R., Arthur, J., Bionta, R., Bostedt, C., Bozek, J., Brachmann, A., Bucksbaum, P., Coffee, R., Decker, F.J., et al. (2010). First lasing and operation of an ångstrom-wavelength free-electron laser. Nat. Photonics *4*, 641–647.
49. Liu, S., Decking, W., Kocharyan, V., Saldin, E., Serkez, S., Shayduk, R., Sinn, H., and Geloni, G. (2019). Preparing for high-repetition rate hard x-ray self-seeding at the European X-ray Free Electron Laser: Challenges and opportunities. Phys. Rev. Accel. Beams *22*, 060704.
50. Küpper, J., Stern, S., Holmegaard, L., Filsinger, F., Rouzée, A., Rudenko, A., Johnsson, P., Martin, A.V., Adolph, M., Aquila, A., et al. (2014). X-ray diffraction from isolated and strongly aligned gas-phase molecules with a free-electron laser. Phys. Rev. Lett. *112*, 083002.
51. Minitti, M.P., Budarz, J.M., Kirrander, A., Robinson, J., Lane, T.J., Ratner, D., Saita, K., Northey, T., Stankus, B., Cofer-Shabica, V., et al. (2014). Toward structural femtosecond chemical dynamics: imaging chemistry in space and time. Faraday Discuss *171*, 81–91.
52. Minitti, M.P., Budarz, J.M., Kirrander, A., Robinson, J.S., Ratner, D., Lane, T.J., Zhu, D., Glownia, J.M., Kozina, M., Lemke, H.T., et al. (2015). Imaging molecular motion: femtosecond x-ray scattering of an electrocyclic chemical reaction. Phys. Rev. Lett. *114*, 255501.
53. Budarz, J.M., Minitti, M.P., Cofer-Shabica, D.V., Stankus, B., Kirrander, A., Hastings, J.B., and Weber, P.M. (2016). Observation of femtosecond molecular dynamics via pump–probe gas phase x-ray scattering. J. Phys. B Atom. Mol. Opt. Phys. *49*, 034001.
54. Stankus, B., Yong, H., Ruddock, J., Ma, L., Carrascosa, A.M., Goff, N., Boutet, S., Xu, X., Zotev, N., Kirrander, A., et al. (2020). Advances in ultrafast gas-phase x-ray scattering. J. Phys. B Atom. Mol. Opt. Phys. *53*, 234004.
55. Stankus, B., Budarz, J.M., Kirrander, A., Rogers, D., Robinson, J., Lane, T.J., Ratner, D., Hastings, J., Minitti, M.P., and Weber, P.M. (2016). Femtosecond photodissociation dynamics of 1,4-diiodobenzene by gas-phase X-ray scattering and photoelectron spectroscopy. Faraday Discuss *194*, 525–536.
56. Glownia, J.M., Natan, A., Cryan, J.P., Hartsock, R., Kozina, M., Minitti, M.P., Nelson, S., Robinson, J., Sato, T., van Driel, T., et al. (2016). Self-Referenced Coherent Diffraction X-Ray Movie of Ångstrom- and Femtosecond-Scale Atomic Motion. Phys. Rev. Lett. *117*, 153003.
57. Stankus, B., Yong, H., Zotev, N., Ruddock, J.M., Bellshaw, D., Lane, T.J., Liang, M., Boutet, S., Carbajo, S., Robinson, J.S., et al. (2019). Ultrafast X-ray scattering reveals vibrational coherence following Rydberg excitation. Nat. Chem. *11*, 716–721.
58. Ware, M.R., Glownia, J.M., Al-Sayyad, N., O'Neal, J.T., and Bucksbaum, P.H. (2019). Characterizing dissociative motion in time-resolved x-ray scattering from gas-phase diatomic molecules. Phys. Rev. *100*, 033413.
59. Yong, H., Moreno Carrascosa, A., Ma, L., Stankus, B., Minitti, M.P., Kirrander, A., and Weber, P.M. (2021). Determination of excited state molecular structures from time-resolved gas-phase X-ray scattering. Faraday Discuss *228*, 104–122.
60. Yong, H., Xu, X., Ruddock, J.M., Stankus, B., Carrascosa, A.M., Zotev, N., Bellshaw, D., Du, W., Goff, N., Chang, Y., et al. (2021). Ultrafast X-ray scattering offers a structural view of excited-state charge transfer. Proc. Natl. Acad. Sci. USA *118*, e2021714118.
61. Yong, H., Zotev, N., Ruddock, J.M., Stankus, B., Simmermacher, M., Carrascosa, A.M., Du, W., Goff, N., Chang, Y., Bellshaw, D., et al. (2020). Observation of the molecular response to light upon photoexcitation. Nat. Commun. *11*, 2157.
62. Ruddock, J.M., Zotev, N., Stankus, B., Yong, H., Bellshaw, D., Boutet, S., Lane, T.J., Liang, M., Carbajo, S., Du, W., et al. (2019). Simplicity Beneath Complexity: Counting Molecular Electrons Reveals Transients and Kinetics of Photodissociation Reactions. Angew. Chem. Int. Ed. *58*, 6371–6375.
63. Ruddock, J.M., Yong, H., Stankus, B., Du, W., Goff, N., Chang, Y., Odate, A., Carrascosa, A.M., Bellshaw, D., Zotev, N., et al. (2019). A deep UV trigger for ground-state ring-opening dynamics of 1,3-cyclohexadiene. Sci. Adv. *5*, eaax6625.
64. Yong, H., Ruddock, J.M., Stankus, B., Ma, L., Du, W., Goff, N., Chang, Y., Zotev, N., Bellshaw, D., Boutet, S., et al. (2019). Scattering off molecules far from equilibrium. J. Chem. Phys. *151*, 084301.
65. Yang, J., Guehr, M., Shen, X., Li, R., Vecchione, T., Coffee, R., Corbett, J., Fry, A., Hartmann, N., Hast, C., et al. (2016). Diffractive Imaging of Coherent Nuclear Motion in Isolated Molecules. Phys. Rev. Lett. *117*, 153002.
66. Yang, J., Zhu, X., Wolf, T.J.A., Li, Z., Nunes, J.P.F., Coffee, R., Cryan, J.P., Gühr, M., Hegazy, K., Heinz, T.F., et al. (2018). Imaging CF3I Conical Intersection and Photodissociation Dynamics with Ultrafast Electron Diffraction. Science *361*, 64–67.
67. Wolf, T.J.A., Sanchez, D.M., Yang, J., Parrish, R.M., Nunes, J.P.F., Centurion, M., Coffee, R., Cryan, J.P., Gühr, M., Hegazy, K., et al. (2019). The Photochemical Ring-Opening of 1,3-Cyclohexadiene Imaged by Ultrafast Electron Diffraction. Nat. Chem. *11*, 504–509.
68. Liu, Y., Sanchez, D.M., Ware, M.R., Champenois, E.G., Yang, J., Nunes, J.P.F., Attar, A., Centurion, M., Cryan, J.P., Forbes, R., et al. (2023). Rehybridization Dynamics into the Pericyclic Minimum of an Electrocyclic Reaction Imaged in Real-Time. Nat. Commun. *14*, 2795.
69. Razmus, W.O., Acheson, K., Bucksbaum, P., Centurion, M., Champenois, E., Gabalski, I., Hoffman, M.C., Howard, A., Lin, M.F., Liu, Y., et al. (2022). Multichannel Photodissociation Dynamics in CS2 Studied by Ultrafast Electron Diffraction. Phys. Chem. Chem. Phys. *24*, 15416–15427.
70. Yang, J., Zhu, X., F Nunes, J.P., Yu, J.K., Parrish, R.M., Wolf, T.J.A., Centurion, M., Gühr, M., Li, R., Liu, Y., et al. (2020). Simultaneous Observation of Nuclear and Electronic Dynamics by Ultrafast Electron Diffraction. Science *368*, 885–889.
71. Champenois, E.G., List, N.H., Ware, M., Britton, M., Bucksbaum, P.H., Cheng, X., Centurion, M., Cryan, J.P., Forbes, R., Gabalski, I., et al. (2023). Femtosecond Electronic and Hydrogen Structural Dynamics

in Ammonia Imaged with Ultrafast Electron Diffraction. Phys. Rev. Lett. *131*, 143001.

72. Kling, M.F., and Vrakking, M.J.J. (2008). Attosecond electron dynamics. Annu. Rev. Phys. Chem. *59*, 463–492.
73. Nisoli, M., Decleva, P., Calegari, F., Palacios, A., and Martín, F. (2017). Attosecond electron dynamics in molecules. Chem. Rev. *117*, 10760–10825.
74. Wörner, H.J., Arrell, C.A., Banerji, N., Cannizzo, A., Chergui, M., Das, A.K., Hamm, P., Keller, U., Kraus, P.M., Liberatore, E., et al. (2017). Charge migration and charge transfer in molecular systems. Struct. Dyn. *4*, 061508.
75. Yong, H., Cavaletto, S.M., and Mukamel, S. (2021). Ultrafast valence-electron dynamics in oxazole monitored by x-ray diffraction following a stimulated x-ray Raman excitation. J. Phys. Chem. Lett. *12*, 9800–9806.
76. Moreno Carrascosa, A., Yang, M., Yong, H., Ma, L., Kirrander, A., Weber, P.M., and Lopata, K. (2021). Mapping static core-holes and ring-currents with x-ray scattering. Faraday Discuss *228*, 60–81.
77. Giri, S., Tremblay, J.C., and Dixit, G. (2021). Imaging charge migration in chiral molecules using time-resolved x-ray diffraction. Phys. Rev. *104*, 053115.
78. Moreno Carrascosa, A., Yong, H., Crittenden, D.L., Weber, P.M., and Kirrander, A. (2019). Ab initio calculation of total x-ray scattering from molecules. J. Chem. Theor. Comput. *15*, 2836–2846.
79. Yong, H., Rouxel, J.R., Keefer, D., and Mukamel, S. (2022). Direct monitoring of conical intersection passage via electronic coherences in twisted x-ray diffraction. Phys. Rev. Lett. *129*, 103001.
80. Hemsing, E., Marinelli, A., and Rosenzweig, J.B. (2011). Generating optical orbital angular momentum in a high-gain free-electron laser at the first harmonic. Phys. Rev. Lett. *106*, 164803.
81. Bahrdt, J., Holldack, K., Kuske, P., Müller, R., Scheer, M., and Schmid, P. (2013). First observation of photons carrying orbital angular momentum in undulator radiation. Phys. Rev. Lett. *111*, 034801.
82. Seiboth, F., Kahnt, M., Lyubomirskiy, M., Seyrich, M., Wittwer, F., Ullsperger, T., Nolte, S., Batey, D., Rau, C., and Schroer, C.G. (2019). Refractive hard x-ray vortex phase plates. Opt. Lett. *44*, 4622–4625.
83. Rouxel, J.R., Rösner, B., Karpov, D., Bacellar, C., Mancini, G.F., Zinna, F., Kinschel, D., Cannelli, O., Oppermann, M., Svetina, C., et al. (2022). Hard x-ray helical dichroism of disordered molecular media. Nat. Photonics *16*, 570–574.
84. Keefer, D., Rouxel, J.R., Aleotti, F., Segatta, F., Garavelli, M., and Mukamel, S. (2021). Diffractive imaging of conical intersections amplified by resonant infrared fields. J. Am. Chem. Soc. *143*, 13806–13815.